ECCOMAS Congress 2016
VII European Congress on Computational Methods in Applied Sciences and Engineering
M. Papadrakakis, V. Papadopoulos, G. Stefanou, V. Plevris (eds.)
Crete Island, Greece, 5–10 June 2016

DIRECT AEROACOUSTIC SIMULATION RELATED WITH MODE CHANGE IN A RECORDER

H. Yokoyama[1], R. Hamasuna[1], A. Miki[2], H. Onitsuka[2], and A. Iida[1]

[1] Department of Mechanical Engineering, Toyohashi University of Technology, Aichi 441-8580, Japan
e-mail: h-yokoyama@me.tut.ac.jp

[2] Research & Development Division, Yamaha Corporation, Shizuoka 438-0192, Japan

Keywords: Direct Aeroacoustic Simulation, Recorder, Musical Instruments, Mode Change

Abstract. *In musical instruments, the mode change of radiating sound is related with their quality. To clarify the flow and acoustic fields related with this mode change, we performed direct aeroacoustic simulations of flow and acoustic fields around two actual recorders with different shapes of windway. The computations are based on the compressible Navier-Stokes equations to predict the fluid-acoustic interactions. It is shown that the relationship between the mean velocity at the windway exit and the mode of the radiating sound for the two models is in good agreement with the measured results. The velocity of the mode change depends on the shape and configurations of the windway and edge. Based on the predicted flow fields, the asymmetry of the jet oscillations between in the upward and downward directions is observed in the recorder model for the earlier mode change.*

1 INTRODUCTION

Flue instruments, such as flutes, bamboo flutes, and recorders, consist of an edge ("labium") with which an air jet collides and a resonator (pipe). In the flue instruments, the fluid-acoustic interactions occur [1]. Since the pioneering works of Helmholtz [2] and Rayleigh [3], many researchers have investigated the self-sustained oscillations of flow and sound in flue instruments. Giordano [4] simulated the effects of the chamfers of the windway exit and clarified the position of the edge (with reference to the windway) on the tonal sound. However, the model was made by extruding a two-dimensional cross-section.

In the previous study [5], the authors conducted the aeroacoustic direct simulations for actual recorders with tone holes. The predicted flow and acoustic fields are in good agreement with the measured results by Particle Image Velocimetry (PIV) and a microphone. Those results also clarified the effects of the condition of tone holes on the sound and flow fields and the mechanism by which self-sustained oscillations (including fluid-acoustic interactions) are maintained.

Also, as the jet velocity increases, the mode of the tone jumps to the higher mode [4, 6]. This mode change of radiating sound is related to their quality. However, to the best knowledge of the authors, the effects of the shape and positions of edge and windway on that mode change have not been clarified sufficiently for actual recorders.

In this paper, the aeroacoustic direct simulations are conducted for two different types of Types S (YRA-28BIII : Straight windway) and A (YRA-38BIII : Arch windway) of recorders as shown in Figure 1. The effects of the shape on the flow and sound fields are discussed focusing on the mode change.

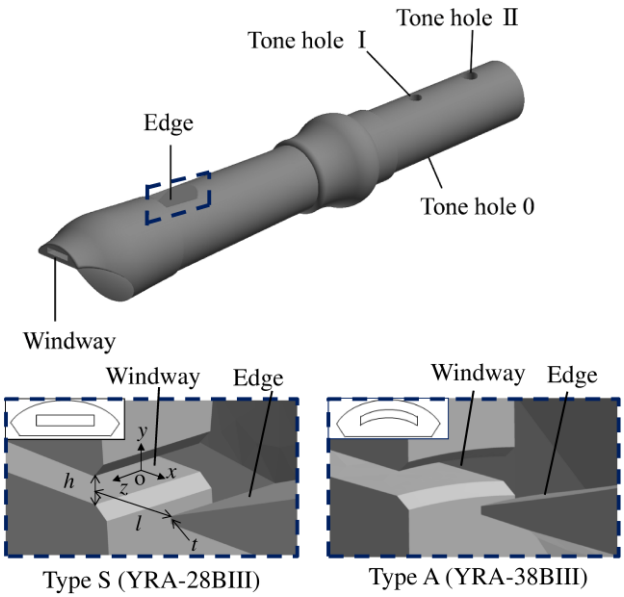

Figure 1: Geometries of recorders.

2 COMPUTATIONAL METHODOLOGIES

2.1 Flow conditions

The flow and acoustic fields around a recorder were investigated by using a short recorder with three tone holes (see Figure 1), namely, actual recorders (Types S and A) cut short after the third hole, as a model. The resonator is conical except in the region near the edge, where

the lower flat surface of the edge is smoothly connected with the circular surface into the resonator. In this paper, the simulations with all tone holes open are discussed.

The origin of the coordinate system of the full model is located at the center of the outlet of the windway. The streamwise direction in the windway is the *x*-axis, the vertical direction is the *y*-axis, and the spanwise direction intersecting with those two axes is the *z*-axis.

Type A and Type S have some different features as shown in Table 1. One difference is the shape of windway exit. The shape is straight and relatively wider (the height h/t = 3.7, where t is the height of the edge and 0.35 mm for both models) for Type S while that is slightly curved (the edge is also curved) and relatively narrower (h/t = 3.0) for Type A. Another difference is the configurations of the windway exit and edge. The distance between the windway exit and the edge, l, (distance of window) for Type S is relatively longer (l/t = 15.0) and the position of the edge with reference to the center of the windway exit, y_e , is relatively higher (y_e/t = -0.29) for Type S, while those are l/t = 13.9 and y_e/t = -0.43 for Type A.

	Windway height h/t	*Distance of window* l/t, l/h	*Edge position* y_e/t, y_e/h
Type S	3.7	15.0, 4.1	-0.29, -0.078
Type A	3.0	13.9, 4.6	-0.46, -0.151

Table 1: Parameters of recorders of Type S and Type A.

The cross-sectional average blow-jet velocity (U_0) is based on the area at the starting point of the chamfers around the exit of the windway. The effects of jet velocity (ranging from 8.0 to 65 m/s) were computationally investigated in the case that all tone holes were open.

2.2 Governing equations and finite-difference formulation

The governing equations used for simulating the interactions between flow and acoustic fields are based on the three-dimensional compressible Navier-Stokes equations. Spatial derivatives are solved by using the sixth-order-accuracy compact finite-difference scheme (fourth-order accuracy at boundaries) [7]. Time integration is performed using the third-order-accuracy Runge-Kutta method.

A volume-penalization (VP) method [8, 9], which is a kind of immersed-boundary method [10], is used to reproduce the flow and acoustic fields around a complex shape of the recorder on a rectangular grid. The penalization term, $\boldsymbol{V}$, is added to right-hand side of the governing equations of the three-dimensional compressible Navier-Stokes equations as follows:

$$\boldsymbol{Q}_t + (\boldsymbol{E} - \boldsymbol{E}_v)_x + (\boldsymbol{F} - \boldsymbol{F}_v)_y + (\boldsymbol{G} - \boldsymbol{G}_v)_z = \boldsymbol{V} \tag{1}$$

$$\boldsymbol{V} = -(1/\phi - 1)\chi \begin{pmatrix} \partial \rho u_i / \partial x_i \\ 0 \\ 0 \\ 0 \\ 0 \end{pmatrix}, \ \phi = 0.25, \tag{2}$$

where $\boldsymbol{Q}_t$ is the vector of the conservative variables, $\boldsymbol{E}$, $\boldsymbol{F}$, and $\boldsymbol{G}$ are inviscid flux vectors, $\boldsymbol{E}_v$ $\boldsymbol{F}_v$, and $\boldsymbol{G}_v$ are viscous flux vectors, and ϕ is the porosity of a porous medium, determined so that the sound wave can be reflected almost completely (reflectivity : 99%). The mask function χ is given as

$$\chi = \begin{cases} 1\,(\text{inside object}) \\ 0\,(\text{outside object}) \end{cases}. \tag{3}$$

To reduce computational cost, large-eddy simulations (LES) were performed for the reproduction of the flow fields in the recorder. In the simulations, no explicit subgrid-scale (SGS) model was used. The turbulent energy in the grid-scale (GS) that should be transferred to SGS eddies is dissipated by a 10th-order spatial filter as described below.

$$\alpha_{\mathrm{f}}\hat{\psi}_{i-1} + \hat{\psi}_i + \alpha_{\mathrm{f}}\hat{\psi}_{i+1} = \sum_{n=0}^{5} \frac{a_n}{2}\left(\psi_{i+n} + \psi_{i-n}\right), \tag{4}$$

where ψ is a conservative quantity and $\hat{\psi}$ is the filtered quantity, also removes numerical instabilities [11]. Coefficient a_n has the same value as that used by Gaitonde and Visbal [12], and the value of α_{f} is 0.45.

The predicted mean and instantaneous flow fields and acoustic fields based on the above-mentioned methodologies have been confirmed to agree with those measured by PIV and a microphone in the previous paper [5].

2.3 Computational domain

The computational domain (shown in Figure 2) is divided into three regions: a vortex region, a sound region, and a buffer region having different grid spacings, while the grid spacing is smoothly changed to prevent spurious acoustic reflections near the boundary of different regions. The computational grid is rectangular (as mentioned above). The total number of grid points is approximately 8.2×10^7. The computational grid is explained in detail in the previous paper [5].

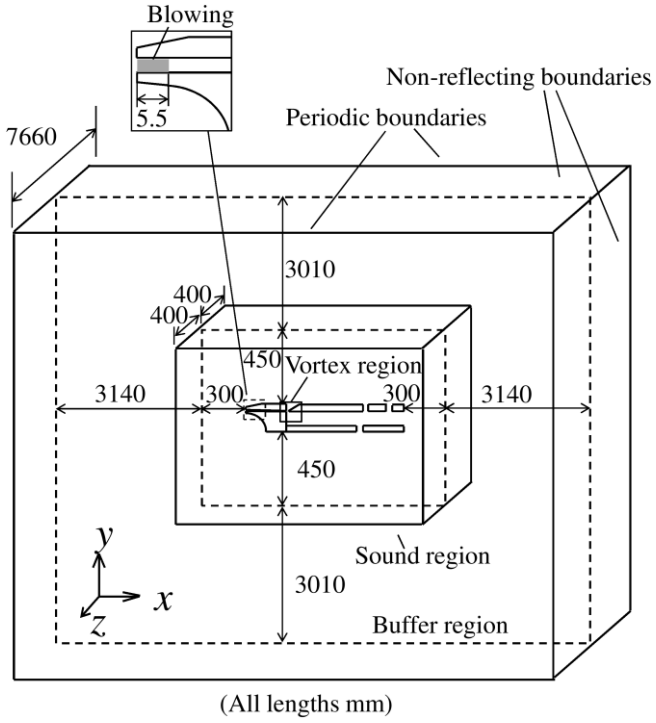

Figure 2: Computational domain and boundary conditions.

2.4 Boundary conditions and initial conditions

The boundary conditions of the computation are shown in Figure 2. Non-reflecting boundaries [13-15] are used at boundaries of the x and y directions, and periodic boundary conditions are adopted in the z direction. To reproduce the jet in the windway, the velocity is set to be a given blowing velocity in the inlet region of the windway, as shown in gray color in Figure 2. For the objects such as a recorder, the above-mentioned mask function is set to $\chi = 1$, and the velocity is set to zero.

In the computation, the velocity is set to zero in the initial field and the jet velocity is accelerated in the duration of computational development.

3 VALIDATION OF COMPUTATIONAL METHODS ABOUT MODE CHANGE

The predicted and measured effects of the jet velocity on the frequency of the dominant tone (fundamental frequency) for Types S and A are shown in Figure 3. As shown in the figure, the predicted frequencies are in good agreement with those measured. As the velocity becomes higher, the frequency of the tonal sound jumps to the second mode. The mode change occurs at a higher velocity for Type A with reference to that for Type S. This difference is also predicted in this simulation as shown in the figure.

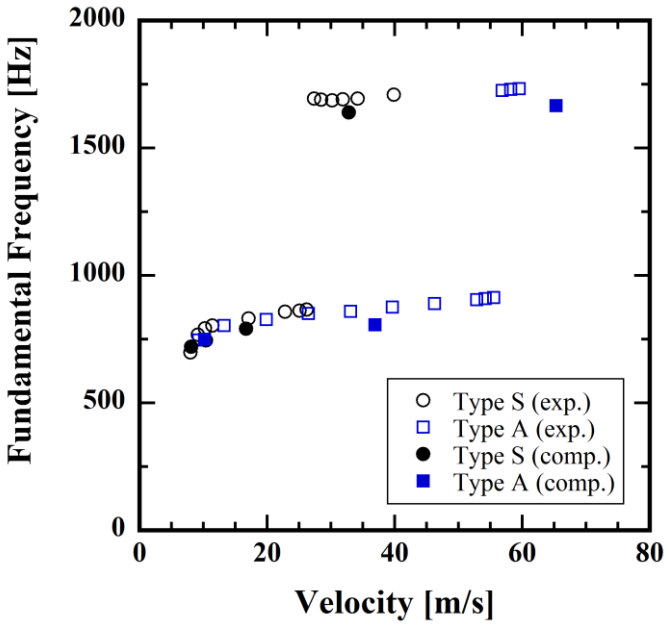

Figure 3: Relationship between the jet velocity U_0 at windway exit and fundamental frequency.

4 RESULTS AND DISCUSSIONS

4.1 Self-sustained oscillations for fundamental mode

Contours of pressure with a time-averaged component subtracted, p', (pressure-fluctuation) and velocity-fluctuation vectors around the exit of the windway and edge at U_0 = 10 m/s in Type S are shown in Figure 4. In the figure, the vectors are shown in the region where the effects of the fluid-dynamical structures (such as vortices) on the fields are small, and the intensity and direction of the acoustic particle velocity are indicated. The time origin (t = 0) is the time that the pressure becomes in the downward region of the edge in fundamental time period T.

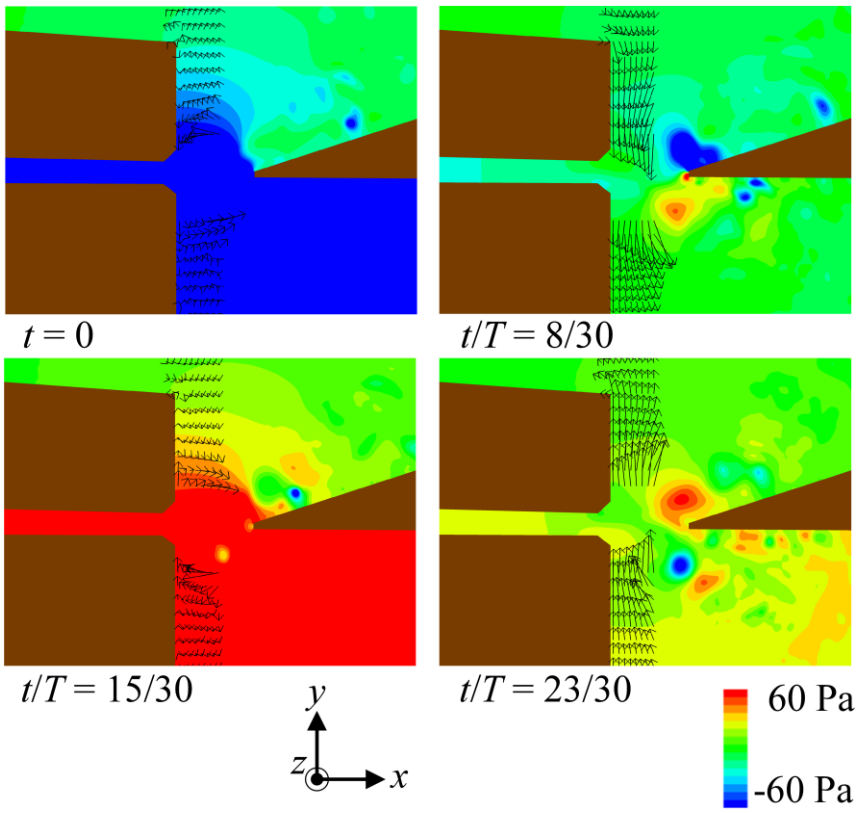

Figure 4 Contours of pressure-fluctuation and velocity-fluctuation vectors (z = 0) at U_0 =10 m/s in Type S, where T is the fundamental time period.

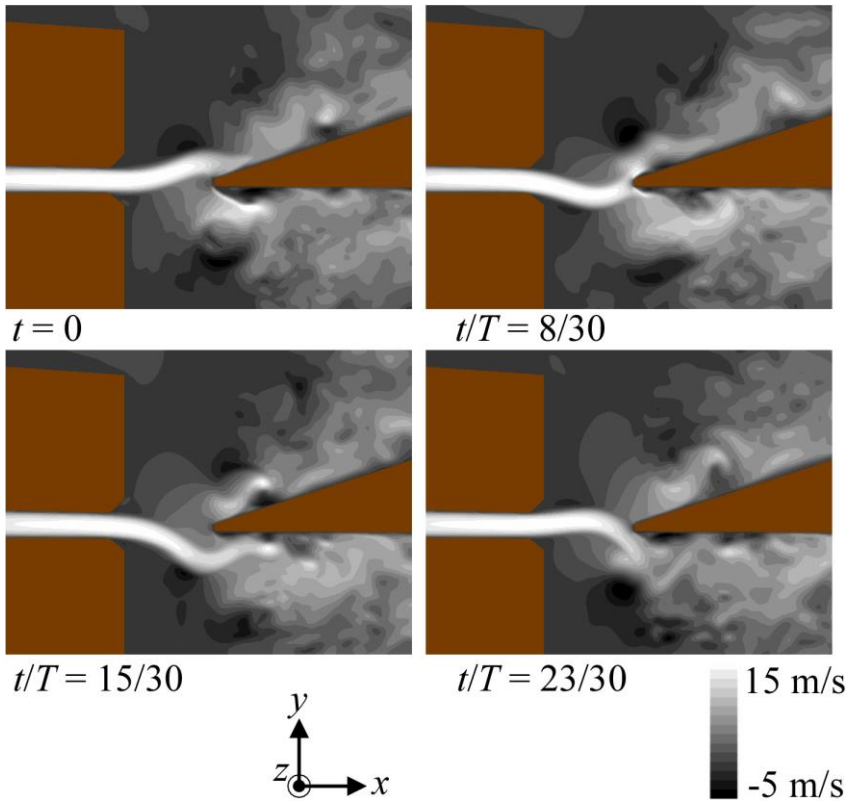

Figure 5 Contours of streamwise velocity (z = 0) at U_0 = 10 m/s in Type S, where T is the fundamental time period.

At t/T = 8/30 in Figure 4, the highest downward particle velocity is induced. Predicted contours of instantaneous streamwise velocity fields are shown in Figure 5. At t/T = 8/30, the jet starts to be deflected downward because the acoustic particle velocity is highest. This mechanism is consistent with experimental results reported by Coltman [16]. Moreover, these small deflections (disturbances) are developed and convected downstream, and as shown in Figure 5, the downward deflection of the jet becomes most intense at t/T = 15/30. As a result, air flows into the resonator on mass and compresses the air in it. In the opposite phase, namely, at t = 0, the air in the resonator expands when the upward deflection of the jet is largest.

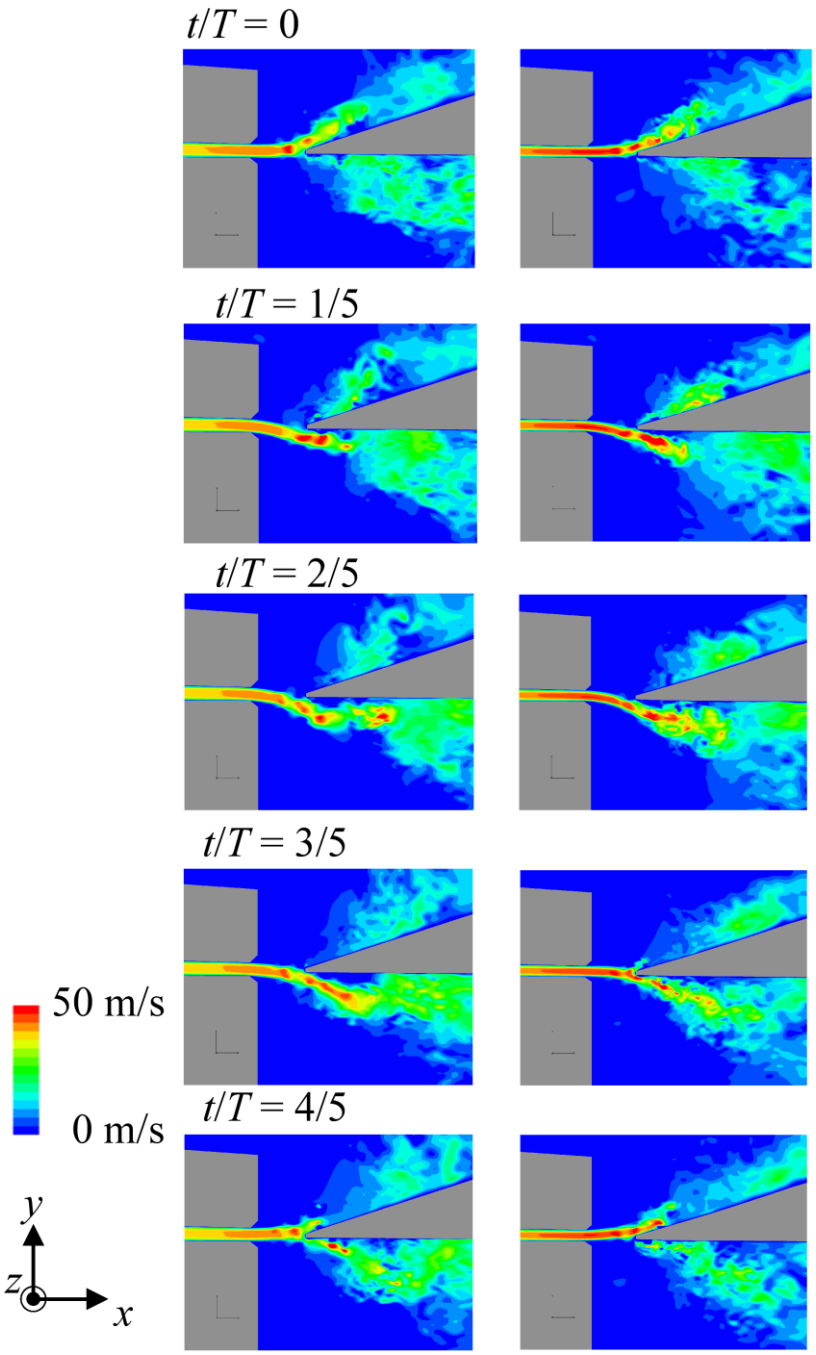

Figure 6 Contours of streamwise velocity (z = 0) at U_0 = 32 m/s in Type S (left) and at U_0 = 35 m/s in Type A (right), where T is fundamental time period.

4.2 Effects of shape on self-sustained oscillations around velocity of mode change

Predicted contours of instantaneous streamwise velocity fields at U_0 = 32 m/s in Type S (left) and at U_0 = 35 m/s in Type A (right) are shown in Figure 6, where the mode change occurs only in Type S.

As shown in the figures, the jet oscillates equally in the upward and downward directions for Type A. However, for Type S, the time in which the jet is inclined in the downward direction is longer than that in the upward direction. This asymmetry of jet oscillations distorts the sound generated by the oscillation of the jets of the fundamental mode, and possibly stimulates the higher mode and the mode change. The position of the edge is relatively higher for Type S as mentioned before, and this is one of the possible reasons why the jet is more likely to be inclined in the downward direction. Giordano [4] also shows that the position of the edge affects the ratios of the power of the fundamental and harmonic tones. Verge [6] also found that the minimum in the generation of the second harmonic was observed when the edge is slightly decentred with respect to the windway exit (y_e = -0.2h). This shift in effective zero transverse position of the edge could be associated with a result of an air entrainment by the jet which can create a static vacuum in the pipe (Coanda effect) and deflect the jet. However, the clear reason why this asymmetry of the jet oscillations is more likely to occur for Type S with comparison to Type A and the relationhip this asymmetry and the mode change are issues that needs further study.

Figure 7 shows the profiles of the mean streamwise velocity at U_0 = 10 and 32 m/s for Type S and at U_0 = 35 m/s for Type A between the windway exit and the edge, where the vertical axis is non-dimensionalized vertical position by the height of the edge, t, with the reference to the position of the center of the edge, y_e.

Comparing between the profiles at U_0 = 10 m/s and those at U_0 = 32 m/s for Type S, it is clarified that the velocity peak is relatively sharper at x/l = 0.5 and 0.75 at U_0 = 32 m/s. This indicates that the smaller amplitude of the oscillations of the jet makes the momentum diffusion smaller at the higher velocity of U_0 = 32 m/s. The variation of the position of the peak velocity along the streamwise position, x, in this figure also shows that the jet is inclined into the downward of the edge at U_0 = 32 m/s for Type S particularly in the profiles with $x/l \geq$ 0.5, while the jet approximately straightly collides with the edge and the jet oscillations are symmetry for Type A. This inclination is due to the asymmetry of the jet oscillations as mentioned above.

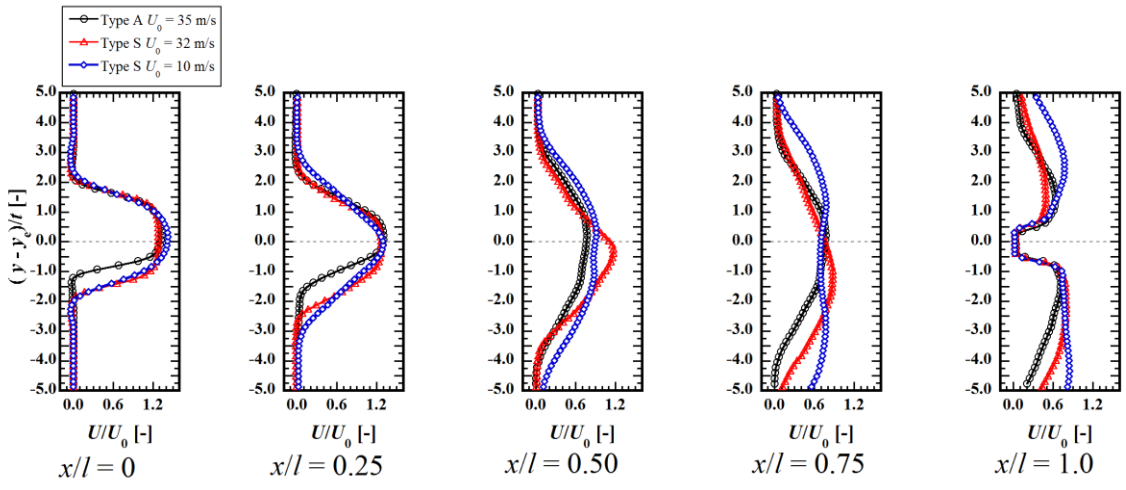

Figure 7 Profiles of mean streamwise velocity (x/l = 0.8) at U_0 = 10 and 32 m/s in Type S and at U_0 = 35 m/s in Type A.

The contours of the pressure-fluctuation, p', are shown in Figure 8. The right figures show that the fundamental mode (a half-wavelength acoustic mode in the pipe) is still dominant for Type A. Meanwhile, focusing on the figures at t/T = 4/5, it can be confirmed that the effects of the second mode (one-wavelength acoustic mode) on the sound fields are more intense for Type S.

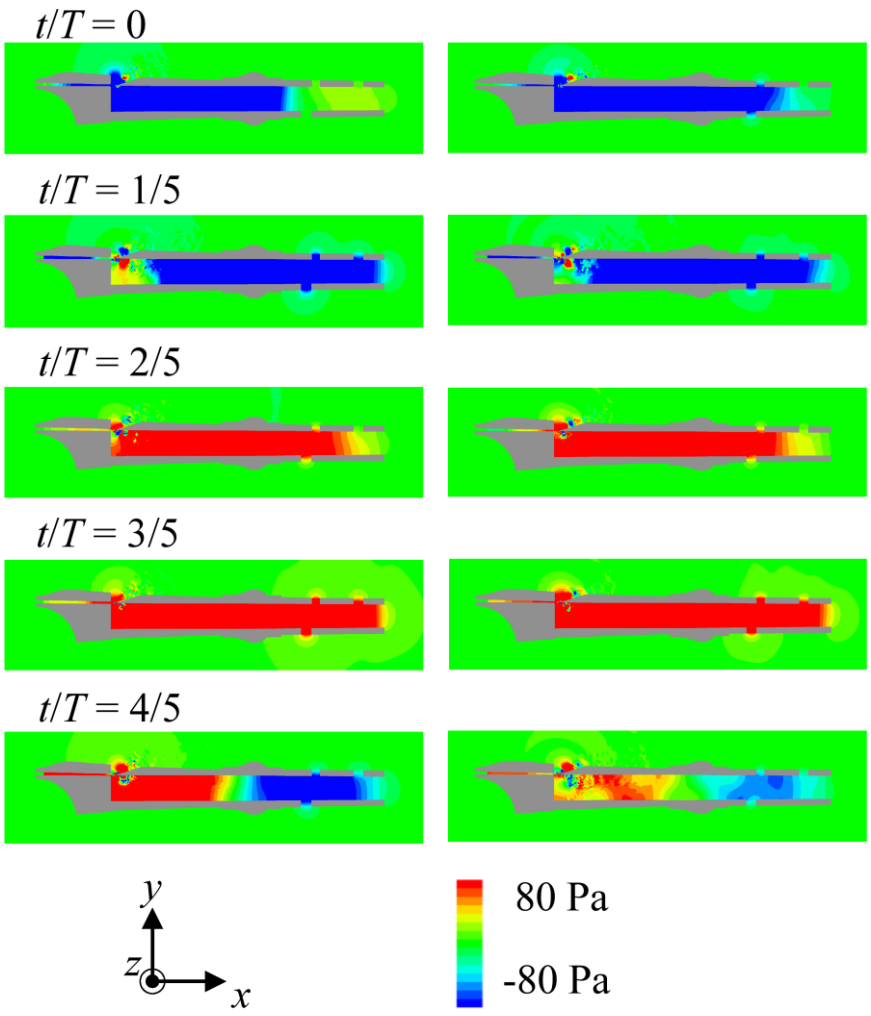

Figure 8 Contours of streamwise velocity (z = 0) at U_0 = 32 m/s in Type S (left) and at U_0 = 35 m/s in Type A (right), where T is the fundamental time period.

5 CONCLUSIONS

Focusing on the mode change of the sound radiating from the recorder, the flow and acoustic fields were predicted with direct aeroacoustic simulations around two actual recorders with different shapes. As a result, the following findings were acquired.

- The present simulations reproduce the mode change of both the recorders, where the velocity for the mode change depends on the configurations and shapes of the windway and edge.
- The asymmetry of the jet oscillations between in the upward direction and in the downward direction was observed only in the recorder model of the earlier mode change.

ACKNOWLEDGEMENTS

The present study was supported by JSPS KAKENHI Grant of No. 26820044 and through the Next-generation Supercomputer Strategy Program by the Ministry of Education, Culture, Sports, Science, and Technology of Japan (MEXT).

REFERENCES

[1] B. Fabre, J. Gilbert, A. Hirschberg, and X. Pelorson, "Aeroacoustics of musical instruments", *Annual Review Fluid Mechanics*, **44**, 1-25, 2012.

[2] H. von Helmholtz, *On the Sensation of Tones*, translated by A. J. Ellis (Dover, New York, 1954), 88-94.

[3] L. Rayleigh (J. W. Strutt), *The Theory of Sound* (Dover, New York, 1945), Vol. 2, Chap. 21.

[4] N. Giordano, "Simulation studies of a recorder in three dimensions", *Journal of the Acoustical Society of America*, **135** (2), 906-916, 2014.

[5] Y. Hiroshi, A. Miki, H. Onitsuka, and A. Iida, *Direct numerical simulation of fluid-acoustic interactions in a recorder with tone holes, Journal of the Acoustical Society of America,* **138** (2), 858-873, 2015.

[6] M. P. Verge, B. Fabre, A. Hirschberg, A. P. J. Wijnands, "Sound production in recorder-like instrument. I. Dimensionless amplitude of the internal acoustic field," *Journal of the Acoustical Society of America*, **101** (5), 2914-2924, 1997.

[7] S. K. Lele. "Compact finite difference schemes with spectral-like resolution," *Journal of Computational Physics*, **103**, 16-42, 1992.

[8] P. Angot, CH Bruneau, and P. Frabrie, "A penalization method to take into account obstacles in viscous flows," Numerische Mathematik **81** (4), 497–520, 1999.

[9] Q. Liu and O. V. Vasilyev, "A Brinkman penalization method for compressible flows in complex geometries", *Journal of Computational Physics*, **227**, 946-966, 2007.

[10] R. Mittal and G. Iaccarino, "Immersed boundary methods," *Annual Review Fluid Mechanics*, **37**, 239-261, 2005.

[11] K. Matsuura and C. Kato, "Large-eddy simulation of compressible transitional flows in a low-pressure turbine cascade," *AIAA Journal*, **45**, 442-457, 2007.

[12] D. V. Gaitonde and M. R. Visbal, "Pade-type higher-order boundary filters for the Navier-Stokes equations," *AIAA Journal*, **38**, 2103-2112, 2000.

[13] K. W. Thompson, "Time dependent boundary conditions for hyperbolic systems," *Journal of Computational Physics*, **68**, 1-24, 1987.

[14] T. J. Poinsot and S. K. Lele, "Boundary conditions for direct simulations of compressible viscous flows," *Journal of Computational Physics*, **101**, 104-129, 1992.

[15] J. W. Kim and D. J. Lee, "Generalized characteristic boundary conditions for computational aeroacoustics," *AIAA Journal*, **38** (11), 2040-2049, 2000.

[16] J. W. Coltman, "Jet drive mechanism in edge tones and organ pipes," *Journal of the Acoustical Society of America*, **60**, 725-733, 1976.